Surface Enrichment in Polymer Blends Involving Hydrogen Bonding

Yuzhi Duan, Eli M. Pearce,* and T. K. Kwei

Department of Chemical Engineering and Chemistry, Polytechnic University, Six MetroTech Center, Brooklyn, New York 11201

Xuesong Hu, Miriam Rafailovich, and Jonathan Sokolov

Department of Materials Science & Engineering, The State University of New York at Stony Brook, Stony Brook, New York 11794

Kungang Zhou and Steven Schwarz

Department of Physics, Queens College 65-30 Kissena Boulevard, Flushing, New York 11367

Received December 8, 2000; Revised Manuscript Received May 31, 2001

ABSTRACT: A phenolic polysiloxane, poly(4-ethenylphenolmethylsiloxane) (PEPS), that contains the phenolic hydroxyl group as a hydrogen-bond donor has been synthesized via hydrosilylation followed by hydrolysis. It was blended with a number of hydrogen-bond acceptors of different strengths, including poly(4-vinylpyridine) (PVPy) (strong), poly(vinylpyrrolidione) (PVPr) (strong), poly(dimethylacrylamide) (PDMA) (moderate), and poly(styrene-*co*-acrylonitrile) (PSAN) (weak). All blends were miscible in the bulk, as indicated by a single DSC T_g, and were shown to be homogeneous by optical microscopy. XPS measurements demonstrated that all PEPS blends had surface enrichment in PEPS, which has a lower surface energy. AFM images showed that the surface morphology in PVPy/PEPS, PVPr/PEPS, and PDMA/PEPS blends did not differ from that in the bulk, whereas the PSAN/PEPS blend exhibited a different surface structure that consisted of PSAN covered with a thin layer of PEPS. Depth profiling by SIMS was in agreement with the XPS analysis. The results indicated that (1) surface enrichment in hydrogen-bonding polymer blends is governed by the interplay between the difference in the surface energy of the constituents and the bulk thermodynamics and (2) hydrogen-bonding interactions reduce surface enrichment.

Introduction

It has been recognized that many important properties of a polymer are determined by the composition and structure of its surface.[1] Among the surface-sensitive properties are adhesion, wettability, friction, biocompatibility, weathering, and many others. In a multicomponent polymer (copolymer or polymer blend) system, the surface composition can differ greatly from that in the bulk as components of lower surface energy always tend to enrich the surface to minimize the free energy of the system. According to the Gibbs adsorption isotherm, any difference in the surface energy of a multicomponent system, $d\gamma$, could result in a relative enrichment of the air interface in the lower-surface-energy material[2]

$$-d_\gamma = \sum_i \Gamma_i \, d\mu_i \qquad (1)$$

where Γ_i is the surface excess of component i ($\Gamma_i \equiv n_i/A$), A is the surface area, and μ_i is the chemical potential of species i for n_i moles of that component. A lowered equilibrium surface energy, resulting from the placement of the lower-surface-energy component at the surface, is achieved at the cost of maintaining a gradient between the surface and bulk compositions. Surface segregation in polymer blends thus reflects a balance of surface forces and bulk mixing thermodynamics, and theoretical descriptions have been proposed that consider this balance in terms of a mean-field formalism.[3−5]

The first quantitative study of segregation in polymer blends focused on a blend of miscible polystyrene (PS) and poly(vinylmethyl ether) (PVME).[6] The surface energies of these two homopolymers are 29 and 35 dyn/cm for PVME and PS, respectively, and the expectation that this blend should be surface-rich in PVME was confirmed by both X-ray photoelectron spectroscopy (XPS) and surface tension measurements. Schmitt and Gardella[7] made a similar observation in blends of polycarbonate (PC) and poly(dimethylsiloxane) (PDMS), reporting an 8-fold increase in the PDMS concentration at the surface. This was not surprising as it is well-known that silicones have lower surface energies than most other polymers (with the exception of aliphatic fluoropolymers).[8] Surface enrichment has been observed even with very small differences in the surface energy of the blend constituents, as in the case of PS mixed with deuterated PS.[9,10]

A number of factors have been shown to affect surface enrichment. Clark et al.[11] studied poly(ϵ-caprolactone)/poly(vinyl chloride) (PCL/PVC) blends and found that the surface composition was dependent on molecular weight and degree of crystallinity. Volkov et al.[12] found that the surface behavior of poly(propylene oxide)/poly(styrene) (PPO/PS) blends was strongly dependent on the solvent used: no surface segregation of PPO is observed in the PPO/PS blends cast from tetrahydrofuran, whereas the blends cast from chloroform exhibit a high surface enrichment of PPO. In the meantime, surface segregation could be hindered by kinetic factors.

Although surface enrichment in polymer blends has been studied extensively, surface segregation in blends with specific interactions, such as hydrogen bonding,

* To whom correspondence should be addressed.

10.1021/ma002093a CCC: $20.00
Published on Web 08/15/2001

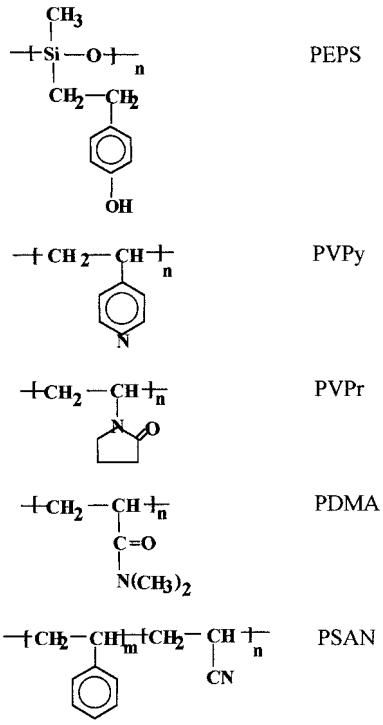

Figure 1. Chemical structures of PEPS and four hydrogen-bond acceptors.

has received little attention. In this work, we have studied the effect of hydrogen-bonding interactions on surface segregation in a series of polymer blends.

We have synthesized a new type of phenolic polysiloxane, poly(4-ethenylphenolmethylsiloxane) (PEPS), based on poly(methylhydrosiloxane). As shown in Figure 1, it contains a flexible siloxane backbone and a terminal hydroxyl group as a hydrogen-bond donor. We prepared PEPS blends by mixing PEPS with a number of polymers that are different in their strengths as hydrogen-bond acceptors, namely, poly(4-vinylpyridine) (PVPy) (strong), poly(vinylpyrrolidione) (PVPr) (strong), poly(dimethylacrylamide) (PDMA) (moderate) and poly(styrene-*co*-acrylonitrile) (PSAN) (weak) (Figure 1). We expected that PEPS would enrich the air/polymer interface of the solvent-cast film because the siloxane backbone would drive it to the interface, thus lowering the interfacial free energy. We also expected that the terminal hydroxyl group would increase the miscibility with hydrogen-bond acceptors. PVPy, PVPr, PDMA, and PSAN were chosen because they all have a characteristic nitrogen atom, while PEPS contains a characteristic atomic silicon, thus simplifying surface analysis by XPS and SIMS. To gain a better perspective on the surface structure of these blends, they were also examined by AFM.

Experimental Section

Materials. Poly(methylhydrosiloxane) (PMHS, $M_n = 2000$) and platinum divinyltetramethyldisiloxane complex (PVMS) were purchased from Gelest Inc. Acetoxystyrene, poly(4-vinylpyridine) (PVPy, $M_n = 29\,200$), poly(dimethylacrylamide) (PDMA, $M_n = 19\,800$), and poly(vinylpyrrolidione) (PVPr, $M_n = 28\,900$) were obtained from Polysciences, Inc. Poly(styrene-*co*-acrylonitrile) (PSAN) copolymers, obtained from the Monsanto Chemicals/Bayer Co., contained acrylonitrile (AN) contents of 24, 26, 29, and 31 wt % and had number-average molecular weights of 83 000, 49 500, 60 900, and 26 000, respectively. Acetoxystyrene was distilled under vacuum.

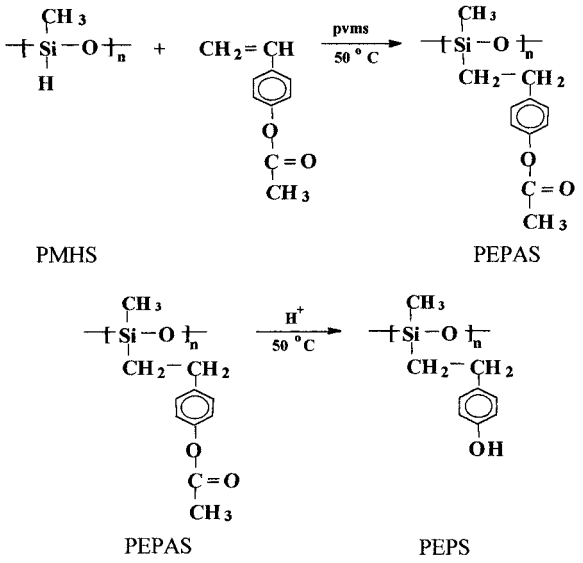

Figure 2. Synthesis of intermediate PEPAS and final product PEPS.

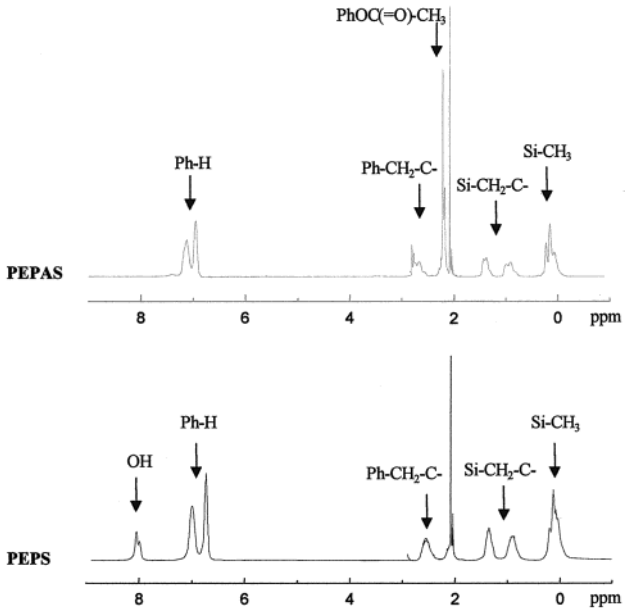

Figure 3. ^{1}H NMR spectra of PEPAS and PEPS.

PMHS, PVPy, PVPr, PDMA, and PSAN copolymers were purified by precipitation before use.

Synthesis. *a. Hydrosilylation.* A mixture of PMHS (2 g; 0.033 mol of Si−H) and acetoxystyrene (0.037 mol, 10% molar excess of PMHS) in dry toluene was degassed with argon. The catalyst PVMS was added to the reaction mixture such that a Pt/acetoxystyrene mole ratio of $1/(5 \times 10^4)$ was obtained. The solution was stirred and heated under reflux at 50 °C until the Si−H absorption peak in the IR spectrum (2170 cm^{-1}) disappeared. The resulting polymer, poly(4-ethenylphenol-acetate methylsiloxane) (PEPAS) (Figure 2), was dissolved in dichloromethane and purified by repeated precipitation with 2-propanol until free from any detectable acetoxystyrene. The polymer was then dried at 40 °C under vacuum for 24 h. ^{1}H NMR (300 MHz, acetone-d_6): $\delta = 0.2$ (Si−CH_3), 0.8−1.4 (Si−CH_2−C−), 2.1 [PhOC(=O)−CH_3], 2.7 (Ph−CH_2−C−), 6.71−7.33 (Ph−H) (Figure 3).

b. Hydrolysis of PEPAS. One gram of PEPAS was dissolved in a mixture of acetone and methanol. The reaction was carried out under argon at 50 °C in the presence of 2 mL of concentrated hydrochloric acid until the carbonyl group absorption peak at 1762 cm^{-1} disappeared. The polymer, poly-

(4-ethenylphenolmethylsiloxane) (PEPS), was recovered by pouring the mixture into excess hexane and was then dried overnight at room temperature under vacuum. ^{1}H NMR (300 MHz, acetone-d_6): δ = 0.2 (Si−CH_3), 0.8−1.4 (Si−CH_2−C−), 2.7 (Ph−CH_2−C−), 6.71−7.33 (Ph−H), 8.05 (OH) (Figure 3).

Sample Preparation. PEPS, PVPy, PVPr, PDMA, and PSAN and their blends were prepared by mixing appropriate amounts of a 2% w/v dimethylformamide (DMF) solution to obtain the desired blend composition. Films were prepared by solvent casting. After being allowed to dry at room temperature, the samples were transferred to a vacuum oven, heated at 110 °C for 70 h, and then cooled to room temperature.

Characterization. The composition of the intermediate PEPAS and the final product PEPS were determined by ^{1}H NMR spectroscopy using a Bruker US-300 spectrometer.

The glass transition temperatures of the polymers and their blends were measured using a Perkin-Elmer DSC 7 instrument. Samples were heated from room temperature to 50 °C below the degradation temperature at a rate of 20 °C/min, cooled to −40 °C, and then scanned again at a rate of 20 °C/min. The glass transition temperature (T_g) was taken as the inflection point of the specific heat jumps observed in the second scan. Thermal degradation of polymers and their blends was investigated with a Perkin-Elmer TGA 7 instrument. The samples were heated to 800 °C at a rate of 20 °C/min under nitrogen.

X-ray photoelectron spectroscopy (XPS) measurements were carried out on a VG Scientific ESCALAB MkII spectrometer using a Mg K_α X-ray source. The spin-coated film on a silicon substrate was mounted on a standard stub by means of double-sided adhesive tape. The X-ray source was run at 12 kV and 10 mA. All spectra were obtained at a takeoff angle of 15° and were curve fitted with Origin 5.1 software.

The surface energy, topography, and friction of polymers and polymer blends were characterized by atomic force microscopy (AFM). Polished silicon(100) wafers were employed as the substrate for AFM measurements. The substrate was dipped in dilute HF solution to remove the silicon oxide on the surface. A thin film of a polymer or polymer blend solution was spin-coated on the substrate. The surfaces were scanned in air using a Digital Dimension 3000 atomic force microscope in contact mode.

Dynamic secondary ion mass spectroscopy (SIMS) measurements of depth profiles of the thin films were carried out on an Atomika 6000 SIMS instrument equipped with a negative argon ion beam rastering the sample surface at an operating voltage of 2 kV and a base pressure of 1.3×10^{-6} Pa. In the dynamic SIMS mode, selected secondary ions were monitored as a function of sputtering time, yielding a concentration vs depth profile.

Fourier transform infrared (FTIR) spectra were recorded with a Nicolet Avatar 400 FTIR spectrometer, with 200 scans at a resolution of 2 cm^{-1}.

The sample thickness of the silicon surface was estimated by ellipsometry. A Rudolph Research Inc. Auto El null-point ellipsometer was used.

Results and Discussion

Miscibility. A common method of assessing the miscibility of a polymer blend is to measure the glass transition temperature of the blend, which represents the onset of the cooperative segmental motion of the component polymers. In a polymer mixture, a single composition-dependent glass transition is commonly taken as an indication of miscibility on the order of 20−40 nm. PEPS blend samples were prepared by mixing 50 mol % PEPS and 50 mol % PVPy, PVPr, PDMA, or PSAN31 in a common solvent, DMF. The mixed solutions of the four polymer blends were all clear. The DSC measurements showed single T_g's for each blend (Table 1), indicating that all four PEPS blends were miscible.

Surface Energy. The traditional method of determining surface energy is contact angle measurement.

Table 1. Bulk Glass Transition Temperatures (T_g) of Individual Polymers and Blends

	PEPS	PVPy	PVPr	PDMA	PSAN31
T_g (°C)	39	150	173	114	109
	–	PVPy/ PEPS50	PVPr/ PEPS50	PDMA/ PEPS50	PSAN31/ PEPS50
T_g (°C)	–	102	110	79	42

Table 2. Adhesive Forces and Surface Energies of Individual Polymers

	PEPS	PVPy	PVPr	PDMA	PSAN31
adhesive force (nN)	18.5	22.8	29.4	37.5	27.3
surface energy (mJ m^{-2})	14.8	22.4	37.2	60.8	32.2

In this work, we determined the surface energies of the polymers by adhesive force measurements via AFM. A nonlinear correlation has been observed between adhesion force and surface energy.[13] El Ghzaoui[14] calculated the surface energies of a series of polymers using the Derjaguin model of a sphere in contact with a flat surface. The calculated surface energy values correlated well with the surface energies measured conventionally by the contact angle method. This method is useful in determining the surface energy of high-energy solids because these solids are often completely wetted by liquid probes, making contact angle measurements meaningless.

According to the Derjaguin approximation, the adhesive force F and surface energy can be correlated by

$$F_{(D=0)} = 4\pi R\sqrt{\gamma_1\gamma_2} \qquad (2)$$

where D is the separation between the tip and the flat surface, R is the radius of the tip and γ_1 and γ_2 are the surface energies of the two bodies in contact. From this expression and adhesive force measurements by AFM, the surface energy of polymers can be determined. Here, γ_1 is the surface energy of the tip, and γ_2 is the surface energy of the polymer of interest. Table 2 lists the adhesive forces and surface energies of PEPS and four hydrogen-bond-accepting polymers determined by AFM. (Note that these surface energies are relative values as the spring constant, radius, and surface energy of the tip were all approximated.)

Note that PEPS has a much lower surface energy than the four other polymers. This implies that, when PEPS is mixed with any of these four polymers, it will preferentially migrate to the surface. Because the driving force for surface enrichment is the difference in surface energy of the two components in a polymer blend,[2] the PEPS blends with higher surface energy differences should show more pronounced surface enrichments in PEPS. Consequently, the order in surface enrichment in PEPS blends from low to high is expected to be PVPy/PEPS < PSAN31/PEPS < PVPr/PEPS < PDMA/PEPS.

Surface Compositions. XPS is based on the kinetic analysis of photoelectrons ejected by the interaction of a molecule with a monoenergetic beam of soft X-rays. XPS is inherently sensitive to the surface because of the very short mean free path of electrons (<100 Å) and its strong dependence on kinetic energy.[15] The XPS-determined surface atomic silicon concentration is representative of polysiloxane PEPS, while the atomic

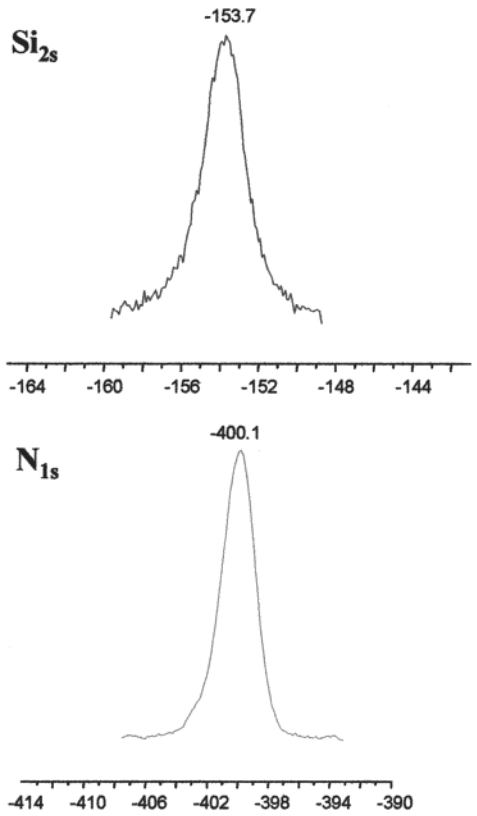

Figure 4. Si_{2s} and N_{1s} core-level spectra for a PVPy/PEPS50 blend.

nitrogen concentration is representative of four hydrogen-bond acceptors, PVPy, PVPr, PDMA, and PSAN31.

The integrated intensity, I_i, of the core−electron photoemmision spectrum is given by[16]

$$I_i \approx S_i N_i \tag{3}$$

where N_i is the average number of atoms per unit sampling volume and S_i is the sensitivity factor. Different elements and different orbitals have different probabilities for interaction with X-ray photons. This results in different sensitivity factors and, thus, different peak areas.

Figure 4 shows the Si_{2s} and N_{1s} XPS spectra of a PVPy/PEPS50 blend measured at a takeoff angle of 15°. The bulk concentrations of PEPS in the samples of the four blends studied were 25, 50, and 75 mol %. Quantitative analysis of the sample surfaces was based on the relation

$$\text{mole \% of PEPS} = \frac{I_{\text{Si2s}}/S_{\text{Si2s}}}{I_{\text{Si2s}}/S_{\text{Si2s}} + I_{\text{N1s}}/S_{N1s}} \tag{4}$$

where I_{Si2s} and S_{Si2s} are the integral peak intensity and sensitivity factor of Si_{2s}, and I_{N1s} and S_{N1s} are the integral peak intensity and sensitivity factor of N_{1s}. The results of the XPS measurements are shown in Table 3.

It is clear that the surface enrichment varies with blend composition, with the only exception being the reversed order of the PSAN31/PEPS50 and PDMA/PEPS50 blends. It is possible that the surface energy difference does not play a significant role in this case. We therefore conclude that the surface enrichment in PEPS blends is influenced not only by the surface energies of the two components but also by the thermodynamic interactions between them. We then proceeded to investigate these interactions by infrared spectroscopy.

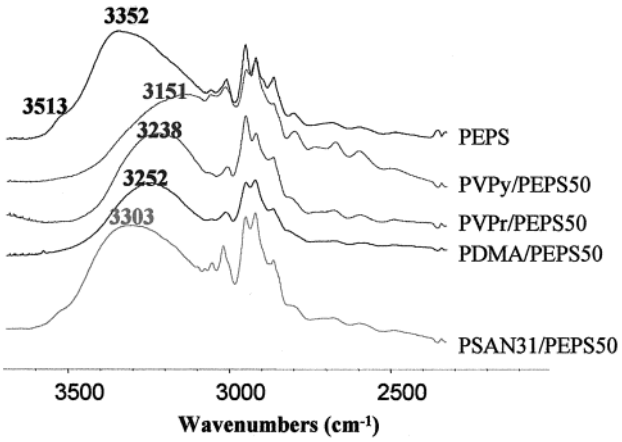

Figure 5. FT-IR spectra of PEPS and its blends in the hydroxyl stretching region.

Table 3. Surface Mole Fractions of PEPS in Blends

bulk mole fraction of PEPS	surface mole fraction of PEPS			
	PVPy/PEPS	PVPr/PEPS	PDMA/PEPS	PSAN31/PEPS
0.25	0.58	0.62	0.66	0.70
0.50	0.67	0.69	0.76	0.85
0.75	0.88	0.89	0.90	0.90

FTIR Spectroscopy. Figure 5 shows the infrared spectra of PEPS and its blends. In the pure PEPS spectrum, there are two types of phenolic OH groups: "free" OH (3513 cm^{-1}) and self-associated OH (3352 cm^{-1}).[17,18] The frequency shift caused by the self-association band is 161 cm^{-1}. After PEPS is mixed with hydrogen-bond acceptors, the absorption band of the free OH shifts to lower wavenumber as a result of intermolecular hydrogen bonding (Figure 5). The large frequency shift suggests a strong intermolecular hydrogen-bonding interaction in PEPS blends.[19] The frequency shifts caused by intermolecular hydrogen-bonding interactions were 362, 275, 261, and 210 cm^{-1} for the PVPy/PEPS50, PVPr/PEPS50, PDMA/PEPS50, and PSAN31/PEPS50 blends, respectively (Table 4), which are greater than the frequency shift for self-associated hydrogen bonding (161 cm^{-1}).

The correlation between the enthalpy of mixing, ΔH_{HB}, and the frequency shift, $\Delta\nu$, when phenol is mixed with a number of hydrogen-bond acceptors is given by eq 5[20]

$$\Delta H_{\text{HB}} = 0.0105\Delta\nu_{\text{OH}} + 2.99 \tag{5}$$

Table 4 lists the calculated hydroxyl group absorption frequency shifts and enthalpies of hydrogen-bond formation in PEPS blends. The magnitude of the frequency shift, and hence the strength of intermolecular hydrogen bonding, in PEPS blends increases in the order PSAN31/PEPS50 < PDMA/PEPS50 < PVPr/PEPS50 < PVPy/PEPS50. Let us make a comparison with the order in surface concentration in PEPS in Table 3. For the PDMA/PEPS50 and PSAN31/PEPS50 blends, the former has a larger frequency shift and heat of mixing but a lower surface enrichment than the latter, which leads to the conclusion that hydrogen-bonding interactions

Table 4. IR Frequency Shifts and Enthalpies of Hydrogen-Bond Formation in PEPS Blends

	PVPy/PEPS50	PVPr/PEPS50	PDMA/PEPS50	PSAN31/PEPS50
frequency shift $\Delta\nu$ (cm^{-1})	362	275	259	210
enthalpy of mixing $-\Delta H_{HB}$ (kJ mol^{-1})	28.4	24.6	23.9	21.7

decrease the surface enrichment in the lower-surface-energy component in polymer blends.

Bulk and Surface Morphology. The bulk morphology of PEPS blends was investigated by optical microscopy. The results showed that all blends were homogeneous (micrographs not shown here). The surface topography was characterized by AFM. The samples were scanned at a rate of 1 Hz using a Si_3N_4 cantilever tip with a force of 10 nN, modulated at 2 kHz with a vertical arm amplitude of 200 Å. The AFM images of the PVPy/PEPS50, PVPr/PEPS50, and PDMA/PEPS50 blend films exhibited a smooth surface (Figure 6a). In contrast, the PSAN31/PEPS50 blend featured two phases on the surface, protruding approximately 2000 Å above the base level (Figure 6b). If this topographical feature was a result of phase separation at the surface, then the regions rich in PSAN31 should have a mechanical response different from that of the rubbery PEPS-rich areas. These expectations were verified by AFM measurements (Figure 7), which showed surface topography and friction images. For the PSAN31/PEPS50 blend, the frictional response of the flat region is greater than that of the higher protrusions (Figure 7d), whereas the other three blends did not show significant frictional contrast (Figure 7b). Thus, we conclude that the elevated regions in the PSAN31/PEPS blend are glassy while the flatter or lower regions are rubbery. As mentioned before, XPS measurements (Table 3) confirm the abundance of PEPS within the top 60 Å of the film surface, which supports the conclusion that the protrusions are the PSAN31-rich phase covered with a thin layer of PEPS because of its high mobility and lower surface energy.

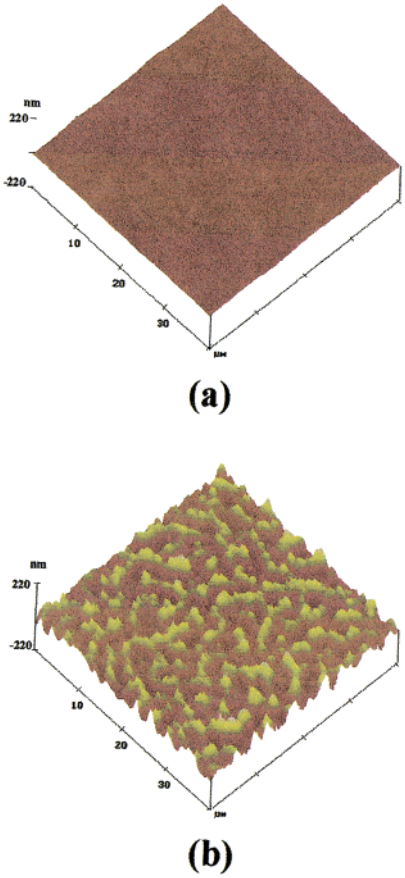

Figure 6. Three-dimensional AFM topographical image of PEPS blend films: (a) PVPy/PEPS50, PVPr/PEPS50, and PDMA/PEPS50; (b) PSAN31/PEPS50.

Surface Depth Profile. SIMS depth profiling was done for the PVPy/PEPS50, PVPr/PEPS50, and PDMA/PEPS50 blends. All of the blends had smooth surfaces, except for the PSAN31/PEPS50 blend. In that blend, phase separation was observed in the AFM images, with one phase protruding about 2000 Å above the base level. Figure 8 shows the raw dynamic SIMS data of a PVPy/PEPS50 sample with 50 mol % PEPS in the bulk that was annealed at 110 °C for 70 h. The thickness of the film was 3000 Å, as measured by ellipsometry. The ion masses analyzed correspond to carbon and silicon. From the data, one can see that the carbon concentration was constant in all layers of the sample and was used as a monitor of the beam current. In this case, the flat carbon trace illustrates the stability of the sputtering beam over a 5-h period, the acquisition time of this spectrum. The depth profile of the pure PEPS sample shows a constant silicon concentration whose intensity was 680 counts. The PEPS surface concentration in the PVPy/PEPS blend was calculated as the silicon intensity in this blend divided by 680.

The other two blends, PVPr/PEPS50 and PDMA/PEPS50, have similar profiles, so they are not shown here. Figure 9 demonstrates an enrichment of PEPS on the surface: 70 mol % PEPS is present at the outermost surface, and the PEPS concentration decreases with depth, in agreement with our XPS measurements.

Dependence of Surface Composition on Bulk Composition. The surface enrichment of PEPS is

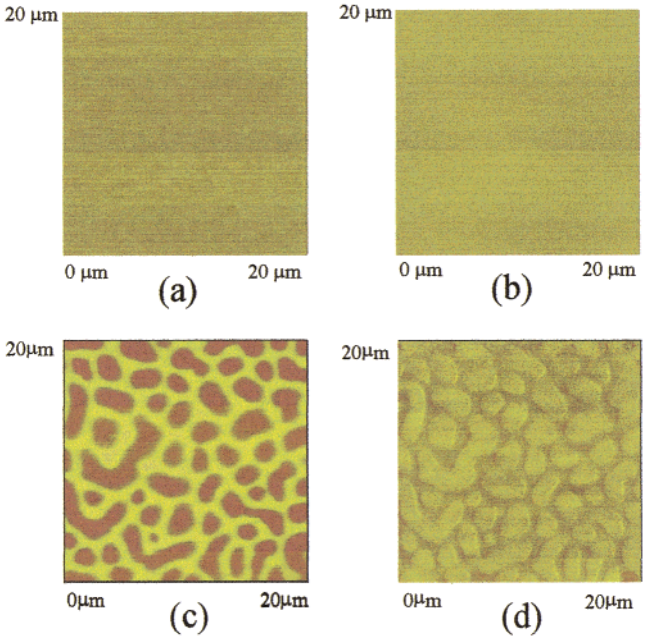

Figure 7. AFM measurements of (a) topography for PVPy/PEPS50, PVPr/PEPS50, and PDMA/PEPS50; (b) friction for PVPy/PEPS50, PVPr/PEPS50, and PDMA/PEPS50; (c) topography for PSAN31/PEPS50; and (d) friction for PSAN31/PEPS50.

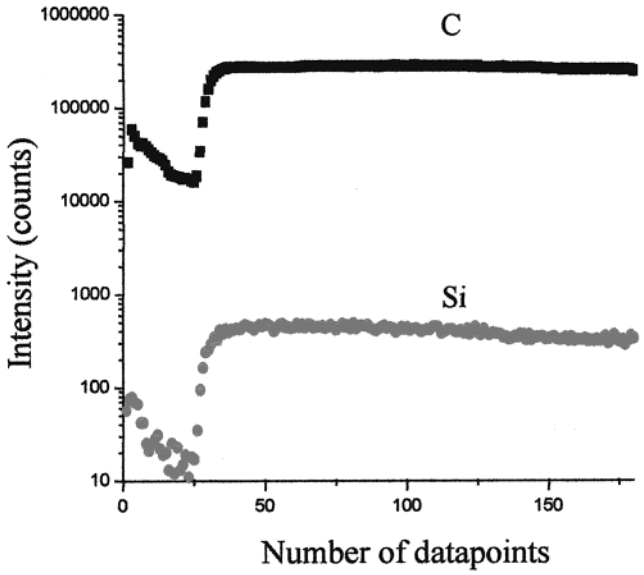

Figure 8. Raw SIMS data of a PVPy/PEPS50 sample annealed at 110 °C for 70 h. The data show scans for C and Si ions.

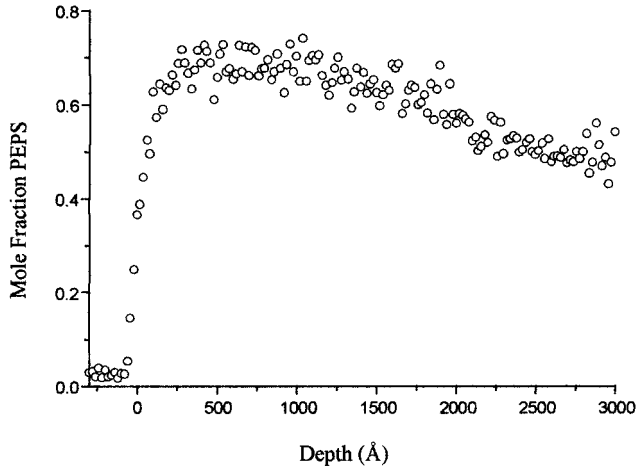

Figure 9. Dynamic SIMS depth profile in PVPy/PEPS50 blend annealed at 110 °C for 70 h.

dependent on the blend constituents and the overall blend composition. This is illustrated in Figure 10 with the PSAN31/PEPS blend as an example. The "average" surface concentration of PEPS is given as a function of the overall blend composition. The average surface concentration reflects the total of all material residing within the sampling depth (~60 Å) in the XPS measurements. An increase in the PEPS bulk concentration in the blend causes a sharp increase in the PEPS surface concentration. For a sample with only 1% bulk PEPS, the surface PEPS concentration reaches up to 35.3%. Between approximately 5 and 30% PEPS bulk concentrations, the surface concentration increases gradually. At about 40% PEPS bulk concentration, the surface concentration increases abruptly before leveling off at 50% bulk concentration. This also indicates the interplay of hydrogen-bonding interactions and surface energy differences on the surface enrichment of PEPS. As shown in Figure 11, with increasing PSAN bulk concentration, i.e., decreasing PEPS concentration, the frequency shift caused by interassociated hydrogen bonding in PEPS/PSAN blends increases, indicating increasing hydrogen-bonding interactions. The frequency shift reaches a maximum at around 40 mol %

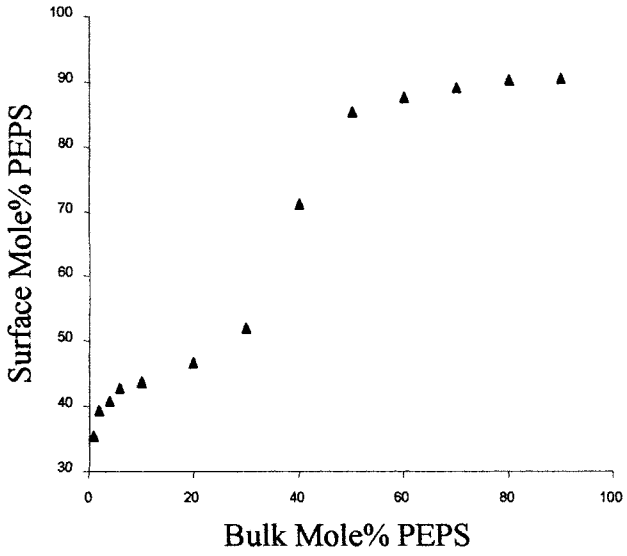

Figure 10. Surface composition dependence in PSAN31/PEPS blends.

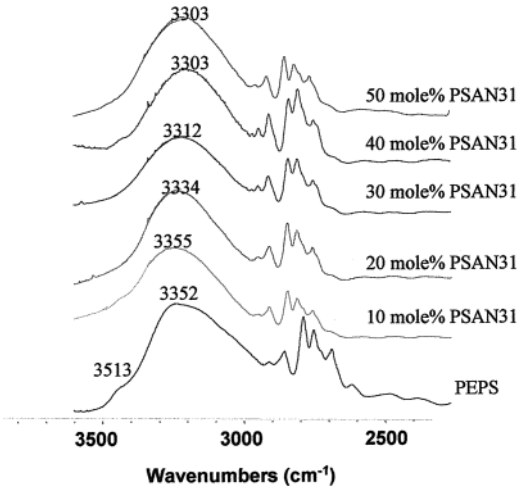

Figure 11. FT-IR spectra of PSAN31/PEPS in the hydroxyl stretching region. The frequency shift $\Delta\nu$ increases with increasing concentration of PSAN31 in the blend.

PSAN concentration, which indicates that the hydrogen-bond density reaches a maximum. When the PEPS concentration is greater than 50 mol %, the surface concentration does not increase with PEPS bulk concentration, and it seems that the surface energy difference dominates in the surface enrichment in PEPS.

On the PEPS surface composition curve, there are two plateaus: the first plateau occurs at a PEPS surface concentration of around 40%, and the second at about 90%. These two plateaus correspond to the PEPS concentrations in the two phases on the surface.

Effect of Hydrogen-Bond Strength. Surface enrichment in polymer blends depends on the balance between the surface energy difference and thermodynamics of mixing. To further explore the effect of hydrogen bonding on surface enrichment, we kept the surface energy difference constant and varied the strength of hydrogen bonding by varying the concentration of acrylonitrile in the PSAN copolymers. The tested polymers include PSAN24, PSAN26, PSAN29, and PSAN31, with acrylonitrile contents of 24, 26, 29, and 31 wt %, respectively. Their surface energies were measured by AFM and are listed in Table 5. The four

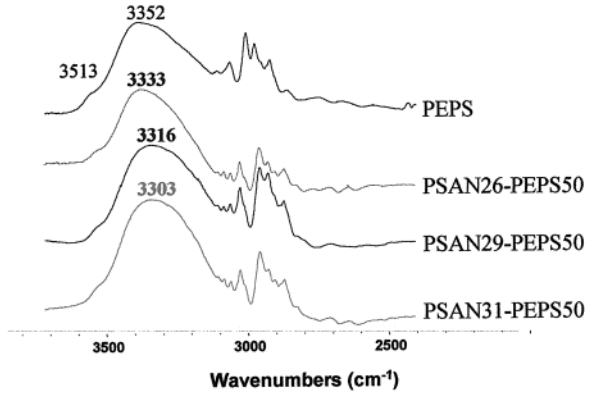

Figure 12. FT-IR spectra of PSAN/PEPS blends in the hydroxyl stretching region: frequency shift $\Delta\nu = 180$ cm^{-1} for PSAN26/PEPS50 blend; $\Delta\nu = 197$ cm^{-1} for PSAN29/PEPS50 blend; $\Delta\nu = 210$ cm^{-1} for PSAN31/PEPS50 blend.

Table 5. Adhesive Forces and Surface Energies of PSAN Copolymers

	PSAN24	PSAN26	PSAN29	PSAN31
adhesive force (nN)	36.9	27.3	27.3	27.3
surface energy (mJ m^{-2})	59.0	32.2	32.2	32.2

Table 6. Surface Mole Fractions of PEPS in PSAN/PEPS Blends

bulk mole fraction of PEPS	surface mole fraction PEPS		
	PSAN26/PEPS	PSAN29/PEPS	PSAN31/PEPS
0.10	0.62	0.53	0.44
0.25	0.70	0.59	0.49
0.50	0.95	0.90	0.85

SAN copolymers have similar surface energies; the sole exception is PSAN24 because of its higher molecular weight, as an increase in polymer surface energy with increasing chain length has been observed.[21] PSAN24 was therefore excluded from the following series of experiments, which employed PSAN26, PSAN29, and PSAN31 blended with 50 mol % PEPS dissolved in DMF. The resulting blends were all clear and showed single DSC T_g indicating miscibility. AFM measurements showed phase separation on the surface of these blend films and an increase in roughness with decreasing acrylonitrile concentration in PSAN.

It was expected that the blend with higher AN content should have stronger hydrogen-bonding interactions and that expectation was verified by infrared spectroscopy. As shown in Figure 12, there is an increase in hydroxyl group absorption frequency shift in these blends with increasing AN content. Hence, the strength of hydrogen bonding in the blends varies in the order PSAN26/PEPS50 < PSAN29/PEPS50 < PSAN31/PEPS50. Table 6 lists the surface compositions of these blends measured by XPS. A surface excess of PEPS is present in these blends and successively decreases with increasing PSAN content, indicating a reduced tendency for surface enrichment by PEPS. We conclude that surface enrichment of the lower-surface-energy component in hydrogen-bonding systems decreases with increasing hydrogen-bonding interactions. Because hydrogen-bonding interactions behave similarly to cross-linking, increasing the strength of hydrogen bonding, i.e., increasing the "cross-linking" density, will decrease the dynamics of chains within the sample. Hence, strongly hydrogen-bonded films are much more stable against internal migration of the polymer components to different interfaces.

Conclusions

We have synthesized and characterized the phenolic polysiloxane poly(4-ethenylphenolmethylsiloxane) (PEPS). The resulting polymer was found to have a very low surface energy and to form miscible blends with strong (PVPy, PVPr), moderate (PDMA), and weak (PSAN) hydrogen-bond acceptors. XPS analysis showed surface enrichment of PEPS for all blends examined, in agreement with depth profiling. The results indicated that (1) surface enrichment in hydrogen-bonding polymer blends responded to changes in the balance between the difference in the surface energies of the constituents and the bulk thermodynamics and (2) hydrogen-bonding interactions reduced surface enrichment.

XPS data for PSAN/PEPS blends showed that the PEPS surface molar concentration increased with increasing PEPS bulk concentration, before reaching saturation at about 50% bulk PEPS concentration. Optical microscopy showed all PEPS blends to be homogeneous in the bulk. AFM micrographs indicated that surface morphology was the same as the bulk morphology for PVPy/PEPS, PVPr/PEPS, and PDMA/PEPS blends but very different from the bulk for PSAN/PEPS blends, which consist of PSAN covered by a thin layer of PEPS on the surface.

Acknowledgment. We thank Dr. Y. Strzhemechny in Queens College for helpful discussions and XPS and SIMS measurements and Drs. Y. Pu and Y. Zhang at SUNY at Stony Brook for help with the AFM measurements.

References and Notes

(1) Andrade, J. D. *Surface Chemistry and Physics*; Plenum Press: New York, 1985.
(2) Defay, R.; Prigogine, I.; Bellemans, A. *Surface Tension and Adsorption*; Wiley: New York, 1951.
(3) Schmitt, I.; Binder, K. *J. Phys.* **1985**, *46*, 1631.
(4) Nakanishi, H.; Pinus, P. *J. Chem. Phys.* **1983**, *79*, 997.
(5) Cohen, M. S.; Muthukumar, J. M. *J. Chem. Phys*, **1989**, *90*, 10.
(6) Bhatia, Q. S.; Pan, D. H.; Koberstein, J. T. *Macromolecules* **1988**, *21*, 2166.
(7) Schmitt, R. L.; Gardella, J. A., Jr. *Macromolecules* **1986**, *19*, 648.
(8) Clarson, S.; Semlyen, J. A. *Siloxane Polymers*; PTR Prentice Hall, Inc.: Englewood Ciffs, NJ, 1993.
(9) Jones, R. A. L.; Kramer, E. J.; Rafailovich, M. H.; Sokolov, J.; Schwarz, S. *Phys. Rev. Lett.* **1989**, *62*, 280.
(10) Jones, R. A. L.; Kramer, E. J. *Philos. Mag. B* **1990**, *62*, 129.
(11) Clark, M. B., Jr.; Burkhardt, C. A.; Gardella, J. A., Jr. *Macromolecules* **1991**, *24*, 799.
(12) Volkov, I. O.; Gorelova, M. M.; Pertsin, A. J.; Filimonova, L. V.; Torres, M. A. P. R.; Oliveriva, C. M. F. *J. Appl. Polym. Sci.* **1988**, *68*, 517.
(13) Good, R. J. *J. Adhes. Sci. Technol.* **1992**, *6* (12), 1269.
(14) El Ghzaoui, A. *J. Appl. Phys.* **1999**, *85* (2), 2000.
(15) Clark, D. T.; Thomas, H. R. *J. Polym. Sci. A: Polym. Chem.* **1977**, *15*, 2843.
(16) Wagner, C. D.; Riggs, W. M.; Davis, L. E.; Moulder, J. F.; Muilenberg, J. E. *Handbook of X-ray Photoelectron Spectroscopy*; Perkin-Elmer: Wellesley, MA, 1979.
(17) Painter, P. C.; Park, Y.; Coleman, M. M. *Macromolecules* **1988**, *21*, 66.
(18) (a) Coleman, M. M.; Graf, J. F.; Painter, P. C. *Specific Interaction and the Miscibility of Polymer Blends*; Technomic Publishing: Lancaster, PA, 1991. (b) Serman, C. J.; Painter, P. C.; Coleman, M. M. *Polymer* **1991**, *32*, 1049.
(19) Coleman, M. M.; Painter, P. C. *Appl. Spectrosc. Rev.* **1984**, *20*, 255.
(20) Lu, S.; Pearce, E. M.; Kwei, T. K. *Polymer* **1995**, *36*, 2435.
(21) Wu, S. *Polymer Interface and Adhesion*; Marcel Dekker: New York, 1960.

MA002093A